Blocking anthrax lethal toxin at the protective antigen channel by using structure-inspired drug design

Vladimir A. Karginov*, Ekaterina M. Nestorovich†, Mahtab Moayeri‡, Stephen H. Leppla‡, and Sergey M. Bezrukov†§

*Innovative Biologics, Inc., 10900 University Boulevard, Manassas, VA 20110; †Laboratory of Physical and Structural Biology, National Institute of Child Health and Human Development, and ‡Bacterial Toxins and Therapeutics Section, National Institute of Allergy and Infectious Diseases, National Institutes of Health, Bethesda, MD 20982

Communicated by John B. Robbins, National Institutes of Health, Bethesda, MD, August 26, 2005 (received for review April 26, 2005)

Bacillus anthracis **secretes three polypeptides: protective antigen (PA), lethal factor (LF), and edema factor (EF), which interact at the surface of mammalian cells to form toxic complexes. LF and EF are enzymes that target substrates within the cytosol; PA provides a heptameric pore to facilitate LF and EF transport into the cytosol. Other than administration of antibiotics shortly after exposure, there is currently no approved effective treatment for inhalational anthrax. Here we demonstrate an approach to disabling the toxin: high-affinity blockage of the PA pore by a rationally designed low-molecular weight compound that prevents LF and EF entry into cells. Guided by the sevenfold symmetry and predominantly negative charge of the PA pore, we synthesized small cyclic molecules of sevenfold symmetry, β-cyclodextrins chemically modified to add seven positive charges. By channel reconstitution and high-resolution conductance recording, we show that per-6-(3-aminopropylthio)-β-cyclodextrin interacts strongly with the PA pore lumen, blocking PA-induced transport at subnanomolar concentrations (in 0.1 M KCl). The compound protected RAW 264.7 mouse macrophages from cytotoxicity of anthrax lethal toxin (= PA + LF). More importantly, it completely protected the highly susceptible Fischer F344 rats from lethal toxin. We anticipate that this approach will serve as the basis for a structure-directed drug discovery program to find new and effective treatments for anthrax.**

infectious diseases | membrane transport | modified cyclodextrins

Anthrax infections are difficult to treat because flu-like symptoms appear only after the bacteria have multiplied inside the human host and started to produce the tripartite toxin that eventually causes death (1, 2). If antibiotics are applied at this stage, the infection can still be lethal because of the accumulation of the toxins. Logically, an effective therapeutic approach would include simultaneous blocking of bacterial growth by antibiotics and neutralization of anthrax toxin with antitoxins (2–5). Extensive research efforts both before and after the anthrax attacks of 2001 have made anthrax toxin one of the best-understood channel-facilitated protein translocation systems (refs. 6–10 and references therein). Protective antigen (83 kDa, PA_{83}) binds to specific cellular receptors, and after being cleaved by a furin-like protease of the host cell into two fragments, PA_{20} and PA_{63}, the latter self-assembles to form a ring-shaped heptameric prepore (11) that can simultaneously bind up to three molecules of lethal factor (LF) and/or edema factor (EF). The complex is then endocytosed and trafficked to an intracellular compartment where acidic conditions induce conversion of the prepore to a pore (9), and EF and LF are translocated into the cytosol presumably by using the PA_{63} channel as a tunnel (12, 13).

Ongoing studies of the anthrax toxin system (summarized in refs. 3 and 9) have yielded promising new approaches to therapy and prophylaxis of anthrax. Therapies under development include toxin-neutralizing antibodies, receptor decoy-based antitoxins, blocking of PA cleavage and oligomerization, and inhibition of LF and EF association with the PA_{63} prepore (3). A polyvalent peptide inhibitor that binds to the heptameric PA_{63} prepore and prevents the interaction between cell-binding and enzymatic moieties has been reported (14). Dominant-negative mutants of protective antigen that co-assemble with the wild-type PA_{63} protein and block its ability to translocate the LF and EF across membranes have also been developed (15). Here we propose another way to prevent LF and EF translocation inside the cell that involves blocking the PA_{63} channel with specially designed low molecular weight compounds. As a starting point for the development of high-affinity blockers of the PA_{63} pore we have used β-cyclodextrin, a cyclic molecule with a hydrophobic cavity.

The idea to use β-cyclodextrin derivatives as inhibitors of anthrax was based on a wealth of earlier research. The high-affinity blockage of transmembrane channels formed by infectious agents has been achieved previously, with probably the most prominent example being the anti-influenza drug amantadine (16). In the particular case of heptameric pores, it was found that the pore of staphylococcal α-hemolysin can be partially blocked by β-cyclodextrin (17) and that tetraalkylammonium cations block the ion conductance of the PA_{63} channel (18), interacting with the negative charges of the PA_{63} pore lumen (11, 19). Guided by these findings, several cationic β-cyclodextrin derivatives as candidate antitoxins were custom-synthesized (20). Here we describe the protective action of one of these compounds, per-6-(3-aminopropylthio)-β-cyclodextrin (AmPrβCD), demonstrated on both single-molecule and whole-organism levels.

Materials and Methods

Chemicals. Recombinant *Bacillus anthracis* LF and PA were produced as described in ref. 21 or acquired from List Biological Laboratories (Campbell, CA). β-Cyclodextrin and 3-[4,5-dimethylthiazol-2-yl]-2,5-diphenyltetrazolium bromide (MTT) were purchased from Sigma, and AmPrβCD was custom synthesized at Pinnacle Pharmaceuticals (Charlottesville, VA). The following chemical reagents were used: KCl, KOH, and HCl (Sigma); EDTA (ResGen); "purum" hexadecane (Fluka); diphytanoyl phosphatidylcholine (Avanti Polar lipids); and pentane (Burdick and Jackson).

Channel Reconstitution. "Solvent-free" bilayer lipid membranes were formed on a 60-μm-diameter (for single-channel measurements) or 150-μm-diameter (for multichannel measurements)

Abbreviations: PA, protective antigen; PA_{83}, 83-kDa PA; LF, lethal factor; EF, edema factor; AmPrβCD, per-6-(3-aminopropylthio)-β-cyclodextrin; LeTx, lethal toxin.

§To whom correspondence should be addressed at: 9000 Rockville Pike, Building 9, Room 1N-124B, National Institute of Child Health and Human Development, National Institutes of Health, Bethesda, MD 20892-0924. E-mail: bezrukos@mail.nih.gov.

aperture in the 15-μm-thick Teflon film that separated two compartments as described elsewhere (22). PA_{63} was prepared from PA_{83} by limited trypsin digestion (23). Single channels were formed by adding 0.5–1 μl of 20 μg/ml stock solution of PA_{63} to 1.5 ml of aqueous phase in the cis half of the chamber. For multichannel experiments we applied 1–2 μl of 0.2 mg/ml stock PA_{63} to the cis side of the membrane. Using this protocol, we have found that PA_{63} insertion was always directional. The applied potential is defined as positive if it is higher at the side of PA_{63} addition.

Cytotoxicity Assays. RAW 264.7 cells (American Type Culture Collection) were grown in DMEM with 10% FCS, 2 mM Glutamax, 2 mM Hepes, and 50 μg/ml gentamycin (all from Invitrogen) at 37°C in a 5% CO_2/95% air atmosphere. Twofold dilutions of compound in DMEM were added to cells for 10 min, followed by addition of medium or lethal toxin (LeTx; PA plus LF) at three different concentrations. Cells treated with LeTx alone, at each of these concentrations, served as positive cytotoxicity controls. Cells treated with medium alone served as negative controls. An additional set of controls involved treatment of cells with drug alone at each concentration to assess drug toxicity. All experiments were done in duplicate. Cells were incubated for 3 h at 37°C, followed by addition of 3-[4,5-dimethylthiazol-2-yl]-2,5-diphenyltetrazolium bromide (MTT) to a final concentration of 0.5 mg/ml. After an additional 45-min incubation, all medium was removed, and cells were dissolved in 50 μl of 0.5% (wt/vol) SDS/25 mM HCl, in 90% (vol/vol) isopropyl alcohol. The plates were vortexed, and the oxidized MTT was measured as A_{570} by using a microplate reader. Percent viability was calculated as a percentage of medium-treated controls. EC_{50} values for protection curves were calculated by using PRISM 4.0 software (GraphPad, San Diego).

Animal Experiments. Male Fischer F344 rats (150 g) (Taconic Farms) were injected intravenously (200 μl) in groups of three with LeTx (10 μg of PA plus 10 μg of LF) in PBS, or in PBS containing AmPrβCD (0.25 mg or 1.25 mg per rat). A separate group of three rats were preinjected with AmPrβCD (1.25 mg per rat, intravenously, in 200 μl of PBS) 30 min before injection of LeTx (10 μg of PA plus 10 μg of LF). Animals were monitored continuously during the first 8 h for signs of malaise and for survival, and twice daily thereafter, for 7 days. All animal experiments were performed according to approved National Institute of Allergy and Infectious Diseases animal care protocols.

Results and Discussion

Seven D-glucose units comprise a β-cyclodextrin molecule (Fig. 1*A Left*) which has sevenfold symmetry (24), like the heptameric PA_{63} prepore (11) (Fig. 1*A Right*), and an outer diameter of ≈15 Å. This diameter is comparable to the PA_{63} prepore internal diameter of 20–35 Å (11) and the diameter of the reconstituted pore, which is at least 11 Å at its most narrow part (25, 26). Advanced methods exist for selective modification of cyclodextrins, and these offer established routes for synthesis of appropriate derivatives (27), for which many pharmaceutical applications have been described (28).

Inhibition of PA_{63} Channels in Planar Lipid Bilayers. We first reconstituted anthrax PA_{63} pores into planar lipid bilayers to study the effects of AmPrβCD on conductance of multichannel membranes and single channels. In both cases we found a profound inhibition of PA_{63}-induced conductance. Fig. 1*B* shows that addition of AmPrβCD to the cis side of a membrane containing ≈60 PA_{63} channels in 0.1 M KCl caused a significant decrease in membrane conductance at extremely low (3 nM) AmPrβCD concentrations. The process advances in a steplike manner (see Fig. 1*B Inset*) with an amplitude of 87 ± 13 pS that coincides with

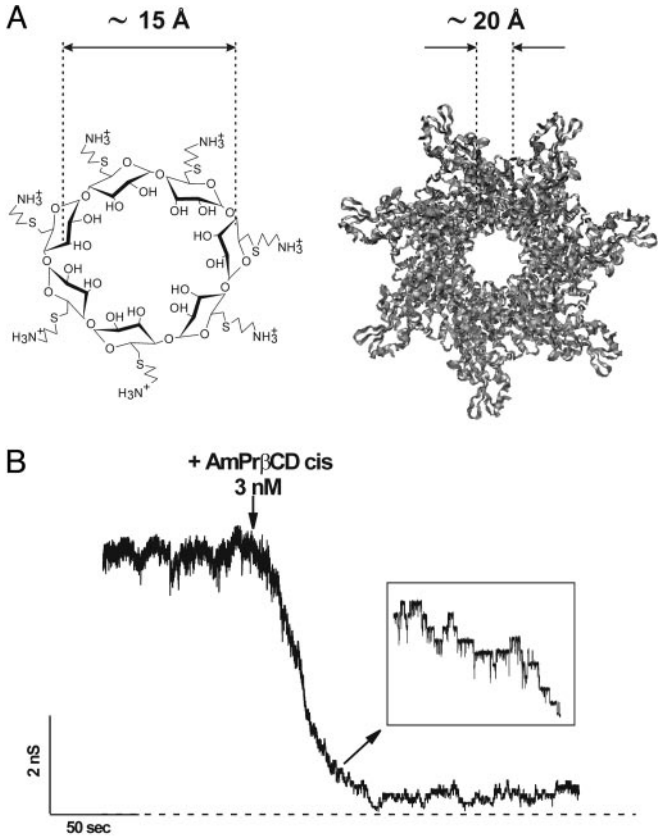

Fig. 1. Schematic illustration of AmPrβCD (*A Left*) in comparison with PA_{63} channel (*A Right*) and its inhibitory action on PA_{63}-induced membrane conductance (*B*). Membrane in *B* contained ≈60 $(PA_{63})_7$ channels. The downward arrow indicates the addition of AmPrβCD to the cis side of the membrane (side of PA addition). The dashed line shows zero current level. The temperature was 23°C and the applied voltage was +20 mV (potential at the cis side of the membrane was more positive). Diphytanoyl phosphatidylcholine planar lipid membranes were bathed by 0.1 M KCl/1 mM EDTA solution at pH 6.6. (Inset) Enlarged (×3) portion of the trace, showing steplike character.

the PA_{63} channel conductance in 0.1 M KCl, showing that AmPrβCD acts on individual channels. Note also that the steady state of multichannel PA_{63} conductance before AmPrβCD addition is rather noisy. This noisiness could be explained by the well known "voltage gating" of PA_{63} channels (25), which tend to stay closed at relatively high voltages but occasionally switch to the closed state even at 20 mV. Moreover, PA_{63} channels exhibit a much faster flickering between the open and closed states (see ref. 18 for details) that also contributes to the fluctuations seen around the steady-state conductance.

Quantitative analysis of the single-channel blockage proved difficult at these physiological salt concentrations because the residence time of the compound in the channel was very long (minutes). Fig. 1*B* (*Inset*) represents the consecutive cutoffs of the channels in a multichannel membrane and the step's lifetime is on the order of seconds. This time, however, reflects only the "on-rate" of the AmPrβCD–PA_{63} association reaction. To be able to obtain reliable statistics on the "off-rate," we switched to 0.3 M and higher salt concentrations. This switch allowed us to more fully characterize and quantify this process on a single-channel level. Typical recordings of ion current through a single PA_{63} pore in 1 M KCl are shown in Fig. 2. A single PA_{63} oligomer spontaneously inserts as an oriented channel showing gating at applied voltages (12, 25) (Fig. 2, topmost track). Addition of 13 nM AmPrβCD to the cis side of the membrane (side of toxin

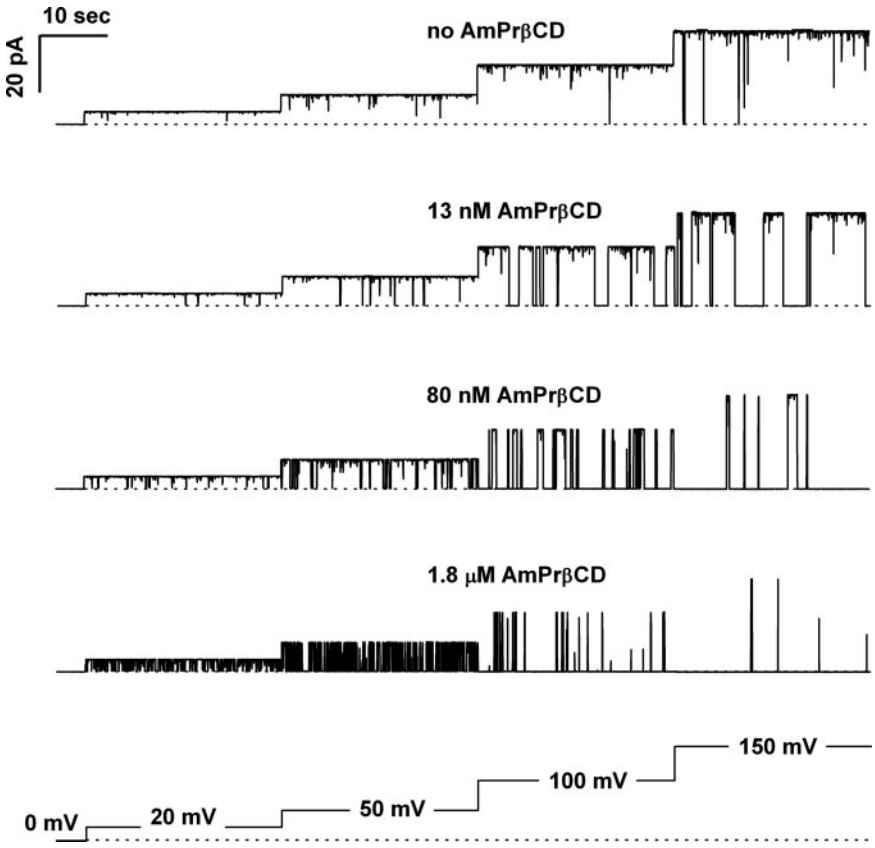

Fig. 2. Modulation of ion current through a single PA_{63} channel by AmPrβCD. Using higher salt concentrations (1 M KCl, pH 6.6), we are able to resolve discrete reversible interruptions in the ion current through a single channel. In the absence of cyclodextrin the ion movement is mainly determined by the geometry and the surface properties of the pore (topmost track). Fast flickering between open and closed states inherent to PA_{63} channels [so-called voltage gating (12, 25)] was mainly removed by averaging over a time interval of 50 msec. In the presence of 13 nM AmPrβCD in the cis half of the chamber, the channel gets spontaneously blocked, and at higher AmPrβCD concentrations (80 nM and 1.8 μM) channel blockages are more frequent.

addition) caused additional fluctuations in the current through a single channel (Fig. 2, second track). These fluctuations are fast transients between a fully open and blocked channel. Increasing the AmPrβCD concentration to 80 nM and 1.8 μM increased the probability of finding the channel in the blocked state (Fig. 2, two lower tracks, and Fig. 3*A*). Note that within the accuracy of our measurements we find that the blockage is complete. It is different, therefore, from the β-cyclodextrin effect on α-hemolysin channels (17), where the blockage is only about 70%.

We found that the binding parameters for this process strongly depend on at least three factors: applied transmembrane voltage (Fig. 3*A*), bathing electrolyte concentration (Fig. 3 *B* and *C*), and lipid charge (data not shown). Fig. 3*A* illustrates the probability of finding the channel in a completely blocked state as a function of voltage at various AmPrβCD concentrations. The probabilities were calculated from the data analogous to that shown in Fig. 2. It is seen that high negative voltages from the side opposite to AmPrβCD addition drag the positively charged AmPrβCD into the channel. We propose that these stepwise transitions reflect the complete blockage of the channel as a result of reversible binding of the positively charged AmPrβCD to the negatively charged residues inside the PA_{63} pore lumen. The involvement of electrostatic interactions is suggested by the strong dependence of blockage parameters on salt concentration. High salt concentrations reduce electrostatic forces significantly, most probably screening out charges on both the blocker and the protein. This screening leads to a decrease in the residence time by orders of magnitude (Fig. 3*C*). In 1 M KCl the "electrical distance" (18) to the blockage site, as calculated from the data in Fig. 3*A* and assuming that AmPrβCD has a charge of +7, is only $\approx$15%.

Fig. 4*A* gives a typical example of a titration curve in a multichannel experiment in 1 M KCl. Fig. 4*B* summarizes inhibition of PA_{63}-induced conductance for three different KCl concentrations: 0.1, 1.0, and 2.5 M. Remarkably, in "physiological" 0.1 M solutions, the 50% inhibitory concentration (IC_{50}) is 0.55 nM. These data are complemented by single-channel analysis that shows a significant increase of AmPrβCD–PA_{63} binding time with lowering of KCl concentration (Fig. 3 *B* and *C*).

Previous studies demonstrated that tetraalkylammonium ions, ranging in size from tetramethylammonium to tetrahexylammonium, reduced membrane macroscopic conductance (>1,000 PA_{63} channels) at micromolar concentrations when added on either the cis (protein-containing) or trans side of the membrane (18, 26). Similar results were recently reported for chloroquine and related compounds (29), which induced multichannel conductance reduction with IC_{50} of $\approx$0.1 μM. In the present work we demonstrate that a rationally designed low molecular weight compound, AmPrβCD, is a 100- to 1,000-fold more potent blocker of anthrax channels [compare IC_{50} of 0.55 nM found in the present study for AmPrβCD with 81 nM for quinacrine (29) and 2.04 μM for pentaalkylammonium (26)].

Exploration of the blockage phenomenon at the level of a single PA_{63} channel with tetrabutylammonium ion (Bu_4N^+) (18) showed that Bu_4N^+ induces blockage of the pore when present on either side of the membrane. The voltage dependence of dwell times allowed the authors to speculate that Bu_4N^+ is driven

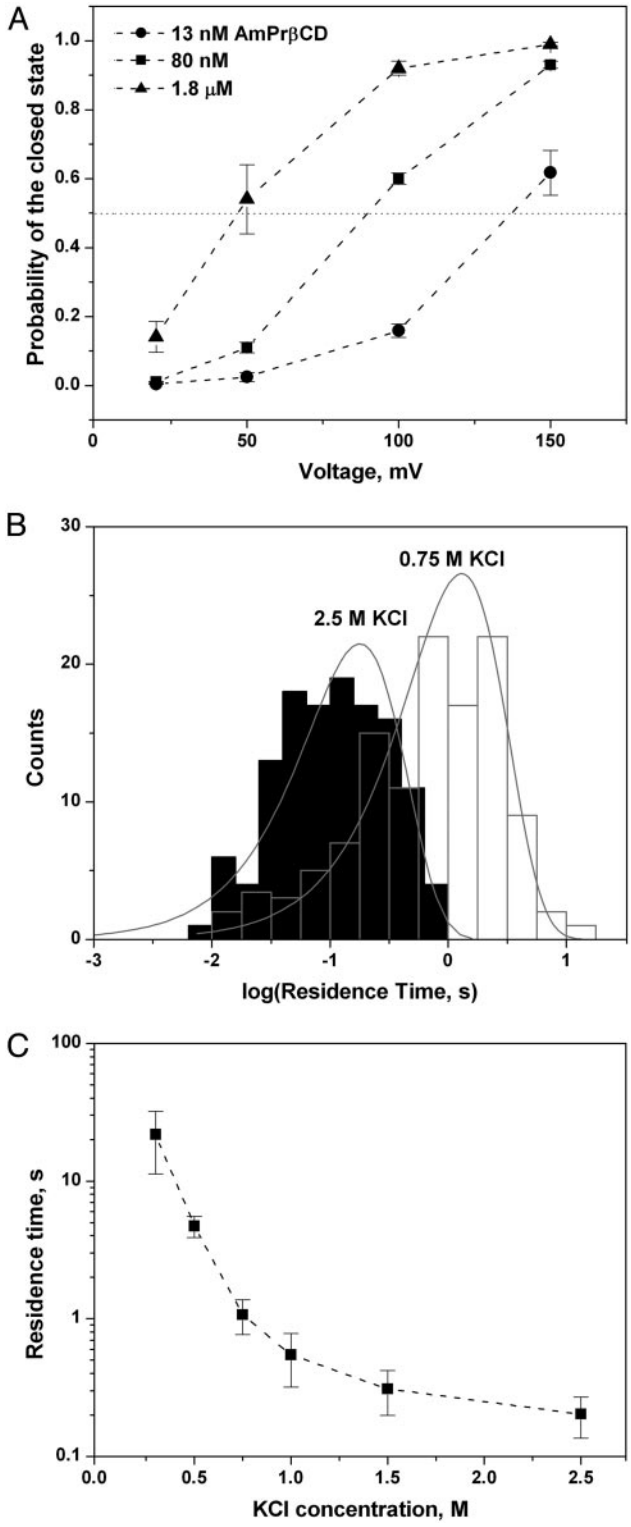

Fig. 3. Kinetic parameters of AmPrβCD binding. (*A*) Higher positive voltages increase the probability to find the channel in a completely blocked state. The probabilities were found as the ratios of the total time spent by the channel in a blocked state to the total observation time. Fifty to 150 blocking events were analyzed, depending on the AmPrβCD concentration and applied voltage. Error bars show root-mean-square deviations of estimates obtained from three different fragments of the current record. (*B*) Typical statistical analyses of AmPrβCD-induced blockages performed by direct single-exponential (''log probability'') fitting of the residence time histograms (see ref. 31 for details of the method). The fits represent ''variable metric'' as a search method and ''maximum likelihood'' as a minimization method. Note the difference in the residence times for 0.75 and 2.5 M KCl. (*C*) Correlation between AmPrβCD residence time and KCl concentration at 100-mV applied voltage. The residence time is obtained by the single-exponential fitting as illustrated in *B*. Error bars represent root-mean-square deviations of estimates obtained by using different search, minimization, and weighting fitting methods available within the CLAMPFIT 9.2.0.10 program (Axon Instruments).

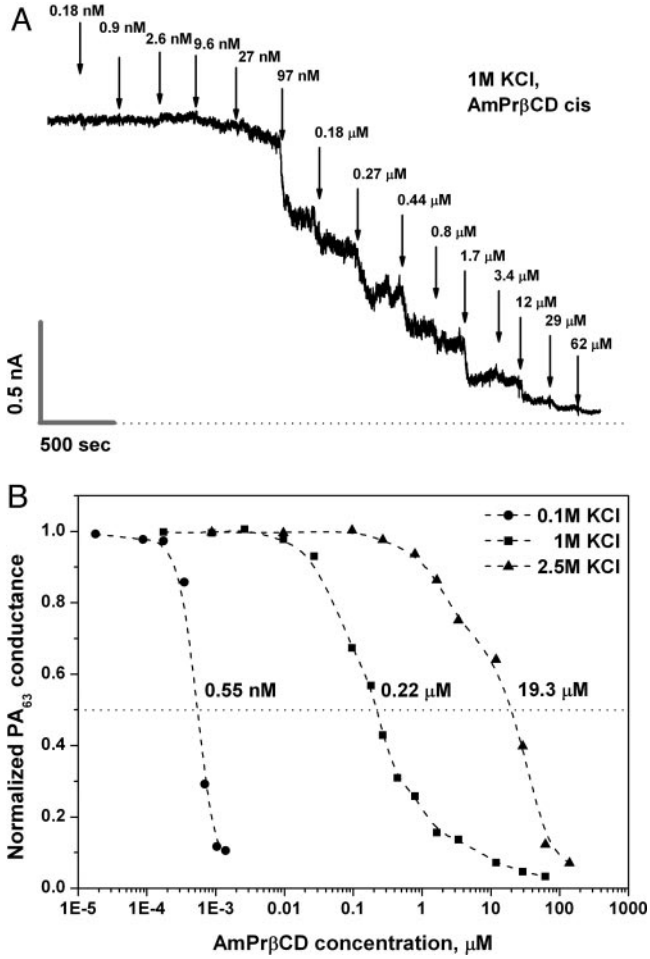

Fig. 4. Multichannel conductance as a function of AmPrβCD concentration in the cis side of the chamber. (*A*) A typical titration curve in 1 M KCl. The current record was filtered by averaging over 500-msec intervals. Certain roughness in the steady-state conductance levels before and after AmPrβCD addition is due to the complicated PA_{63} kinetics as well as the finite number of the channels in the membrane. (*B*) AmPrβCD inhibitory concentration depends on KCl bulk concentration, giving IC_{50} as 0.55 nM, 0.22 μM, and 19.3 μM for 0.1 M, 1.0 M, and 2.5 M KCl solutions, correspondingly. The applied voltage was +20 mV.

through the channel by voltage and binds to the same blocking site within the channel lumen. Correspondingly, we believe that AmPrβCD interrupts the current through the PA_{63} pore as a result of strong interaction of the positively charged amino groups with the negatively charged residues inside the channel. We find that AmPrβCD blocks ion current through the pore very effectively when added to cis, trans, or both sides of the membrane (data not shown). This observation shows that the AmPrβCD molecule is able to enter the channel from both extracellular and intracellular openings.

In comparison with AmPrβCD, the nonmodified neutral β-cyclodextrin displayed only weak binding affinity when added from the trans (intracellular and, therefore, physiologically irrelevant)

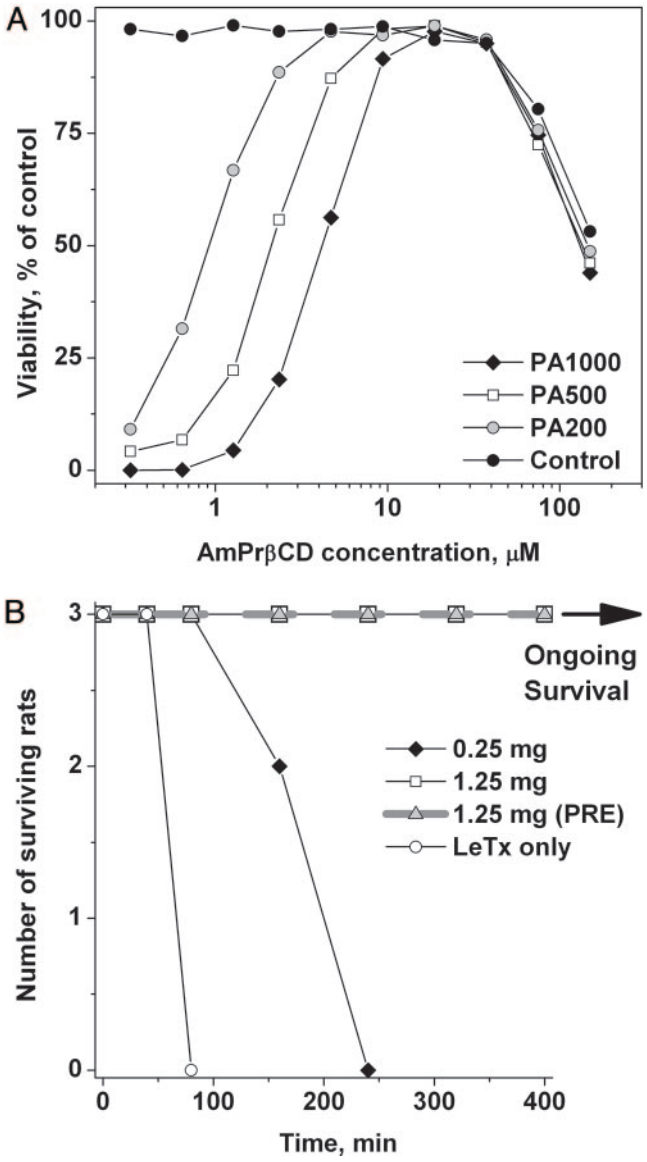

Fig. 5. Protection of RAW 264.7 cells (*A*) and Fischer F344 rats (*B*) from LeTx-induced death by AmPrβCD. (*A*) RAW 264.7 cells were incubated with various concentrations of AmPrβCD and LeTx or medium was added. PA was used at three final concentrations (1000, 500, and 200 ng/ml). LF was constant at a final concentration of 100 ng/ml in all experiments. After 3 h, viability was determined by 3-[4,5-dimethylthiazol-2-yl]-2,5-diphenyltetrazolium bromide (MTT) assay. Percentage viability was calculated relative to cells treated with medium alone. (*B*) Three groups of rats (n = 3 per group) were injected intravenously with 10 μg of LeTx (10 μg of PA plus 10 μg of LF) alone, or mixed with AmPrβCD (0.25 mg or 1.25 mg). A fourth group of rats (n = 3) was pretreated with 1.25 mg of AmPrβCD and injected intravenously with LeTx after 30 min. Survival was monitored for each group continuously over 8 h and periodically for survivors over a period of 7 days.

side of the membrane. According to our experiments (data not shown), the corresponding IC_{50} in 0.1 M KCl solutions is 5–60 μM, depending on the applied voltage. Similarly, β-cyclodextrin binds only weakly to a heptameric α-hemolysin channel (17) and to connexin channels reconstituted in unilamellar liposomes (30). These previous studies showed that the nonmodified β-cyclodextrin can enter the channels and reach its binding site from the cytoplasmic side but not from the side that is normally extracellular. Here we successfully designed and tested a derivative that is able to effectively block PA_{63} channel by entry into the pore lumen from the extracellular side of the membrane.

Inhibition of Lethal Toxin in Cells and Animals. The strong binding of AmPrβCD to the PA_{63} channel demonstrated in the channel reconstitution experiments above implied that the candidate drug would block LeTx action in biological systems. We evaluated the ability of AmPrβCD and nonmodified β-cyclodextrin to inhibit the cytotoxic effect of LeTx on the mouse macrophage-like RAW 264.7 cell line. Macrophages were treated with 2-fold dilutions of either compound for 10 min before addition of set concentrations of LeTx. Medium-treated control cells also received the same LeTx concentrations, which served as positive cytotoxicity controls. Cells treated with medium alone served as negative cytotoxicity controls. Whereas nonmodified β-cyclodextrin did not show protection against LeTx up to 100 μM concentrations, the cationic AmPrβCD protected against LeTx action in a manner dependent on the PA concentration (Fig. 5*A*). The calculated IC_{50} values for AmPrβCD protection against LeTx under the 3-h assay conditions used were 4.25 μM, 1.61 μM, and 0.278 μM for PA concentrations of 1,000 ng/ml (12 nM), 500 ng/ml (6 nM), and 200 ng/ml (2.4 nM), respectively. Controls treated with drug alone indicated that AmPrβCD was not toxic to RAW 264.7 cells up to 37.5 μM but showed increasing toxicity at higher concentrations, with a killing EC_{50} of $\approx$150 μM.

Finally, we evaluated the efficacy of this compound in the highly LeTx-sensitive Fischer F344 rat. Whereas control rats injected with LeTx (10 μg of PA plus 10 μg of LF) died in 77–83 min, rats treated with toxin and AmPrβCD (1.25 mg per rat) were fully protected and showed no signs of malaise (Fig. 5*B*). This amount of compound corresponds to $\approx$40–50 μM in the rat circulation (based on 12–15 ml per rat), whereas the concentration of PA in the animals, based on the same volume, is 8–10 nM, indicating a >1,000-fold molar excess of drug. A 5-fold lower concentration of AmPrβCD was not effective in protecting the rats, although it did extend their survival significantly, to an average of $\approx$200 min (Fig. 5*B*). Interestingly, pretreatment of the rats with 1.25 mg of AmPrβCD 30 min before LeTx challenge was also fully protective. This group of rats, however, showed some signs of malaise, including shortness of breath and lethargic behavior for 6–8 h, before full recovery.

In conclusion, we believe the data presented here illustrate the value of a structure-based drug design that exploits unique features of the target molecule. The oligomeric nature of the central component of anthrax toxin, the PA_{63} heptamer, enabled us to dock to it, with high affinity, a complementary oligomeric compound of low molecular weight. This approach can be extended to the design of inhibitors of other toxins and protein channels that play key roles in the action of pathogenic bacteria.

We are grateful to Adrian Parsegian for valuable discussions and comments. We thank Mr. Jason Wiggins for help with animal experiments. This research was supported by the Intramural Research Program of the National Institutes of Health, National Institute of Child Health and Human Development and National Institute of Allergy and Infectious Diseases and by Grant 1R43AI052894-01 from the National Institute of Allergy and Infectious Diseases.

1. Bartlett, J. G., Inglesby, T. V. & Borio, L. (2002) *Clin. Infect. Dis.* **35,** 851–858.
2. Bull, J. J. & Parrish, C. R. (2002) *Science* **297,** 201–202.
3. Rainey, G. J. & Young, J. A. (2004) *Nat. Rev. Microbiol.* **2,** 721–726.
4. Friedlander, A. M. (2001) *Nature* **414,** 160–161.
5. Karginov, V. A., Robinson, T., Riemenschneider, J., Golding, B., Kennedy, M., Shiloach, J. & Alibek, K. (2004) *FEMS Immun. Med. Microbiol.* **40,** 71–74.
6. Chaudry, G. J., Moayeri, M., Liu, S. & Leppla, S. H. (2002) *Trends Microbiol.* **10,** 58–62.
7. Mourez, M., Lacy, D. B., Cunningham, K., Legmann, R., Sellman, B. R., Mogridge, J. & Collier, R. J. (2002) *Trends Microbiol.* **10,** 287–293.
8. Liu, S., Schubert, R. L., Bugge, T. H. & Leppla, S. H. (2003) *Expert Opin. Biol. Ther.* **3,** 843–853.

9. Collier, R. J. & Young, J. A. (2003) *Annu. Rev. Cell Dev. Biol.* **19,** 45–70.
10. Moayeri, M. & Leppla, S. H. (2004) *Curr. Opin. Microbiol.* **7,** 19–24.
11. Petosa, C., Collier, R. J., Klimpel, K. R., Leppla, S. H. & Liddington, R. C. (1997) *Nature* **385,** 833–888.
12. Blaustein, R. O., Koehler, T. M., Collier, R. J. & Finkelstein, A. (1989) *Proc. Natl. Acad. Sci. USA* **86,** 2209–2213.
13. Zhang, S., Udho, E., Wu, Z., Collier, R. J. & Finkelstein, A. (2004) *Biophys. J.* **87,** 3842–3849.
14. Mourez, M., Kane, R. S., Mogridge, J., Metallo, S., Deschatelets, P., Sellman, B. R., Whitesides, G. M. & Collier, R. J. (2001) *Nat. Biotechnol.* **19,** 958–961.
15. Sellman, B. R., Mourez, M. & Collier, R. J. (2001) *Science* **292,** 695–697.
16. Hay, A. J., Wolstenholme, A. J., Skehel, J. J. & Smith, M. H. (1985) *EMBO J.* **4,** 3021–3024.
17. Gu, L. Q., Braha, O., Conlan, S., Cheley, S. & Bayley, H. (1999) *Nature* **398,** 686–690.
18. Blaustein, R. O., Lea, E. J. A. & Finkelstein, A. (1990) *J. Gen. Physiol.* **96,** 921–942.
19. Benson, E. L., Huynh, P. D., Finkelstein, A. & Collier, R. J. (1998) *Biochemistry* **37,** 3941–3948.
20. Karginov, V. A., Yohannes, A., Tanisha, M., Robinson, T. M., Fahmi, N. E., Alibek, K. & Hecht, S. M. (2005) *Bioorg. Med. Chem.*, in press.
21. Park, S. & Leppla, S. H. (2000) *Protein Expression Purif.* **18,** 293–302.
22. Nestorovich, E. M., Danelon, C., Winterhalter, M. & Bezrukov, S. M. (2002) *Proc. Natl. Acad. Sci. USA.* **99,** 9789–9794.
23. Novak, J. M., Stein, M.-P., Little, S. F., Leppla, S. H. & Fridlander, A. M. (1992) *J. Biol. Chem.* **267,** 17186–17193.
24. Szejtli, J. (1998) *Chem. Rev.* **98,** 1743–1753.
25. Finkelstein, A. (1994) *Toxicology* **87,** 29–41.
26. Blaustein, R. O. & Finkelstein, A. (1990) *J. Gen. Physiol.* **96,** 905–919.
27. Khan, A. R., Forgo, P., Stine, K. J. & D'Souza, V. T. (1998) *Chem. Rev.* **98,** 1977–1996.
28. Davis, M. E. & Brewster, M. E. (2004) *Nat. Rev. Drug Discov.* **3,** 1023–1035.
29. Orlik, F., Schiffler, B. & Benz, R. (2005) *Biophys. J.* **88,** 1715–1724.
30. Locke, D., Koreen, I. V., Liu, J. Y. & Harris, A. L. (2004) *J. Biol. Chem.* **279,** 22883–22892.
31. Sigworth, F. J. & Sine, S. M. (1987) *Biophys. J.* **52,** 1047–1054.